TECHNICAL MEMORANDUM

494

# "1D+4D-Var" assimilation of NCEP Stage IV radar and gauge hourly precipitation data

Philippe Lopez and Peter Bauer

Research Department

Submitted to Monthly Weather Review

July 2006



European Centre for Medium-Range Weather Forecasts
Europäisches Zentrum für mittelfristige Wettervorhersage
Centre européen pour les prévisions météorologiques à moyen terme

Series: ECMWF Technical Memoranda

A full list of ECMWF Publications can be found on our web site under:
http://www.ecmwf.int/publications/

Contact: library@ecmwf.int



European Centre for Medium-Range Weather Forecasts
Shinfield Park, Reading, RG2 9AX, England

**Abstract**

The "1D+4D-Var" assimilation method currently run in operations at ECMWF with rain-affected radiances from the Special Sensor Microwave/Imager is used to study the potential impact of assimilating NCEP Stage IV analyses of hourly accumulated surface precipitation over the United States (US) main land. These data are a combination of rain gauge measurements and observations from the high-resolution Doppler NEXt-generation RADars (NEXRAD). Several "1D+4D-Var" experiments have been run over a month in spring 2005. First, the quality of the precipitation forecasts in the control experiment is assessed. Then, it is shown that the impact of the assimilation of the additional rain observations on global scores of dynamical fields and temperature is rather neutral, while precipitation scores are improved for forecast ranges up to 12 hours. Additional "1D+4D-Var" experiments in which all moisture-affected observations are removed over the US, demonstrate that the NEXRAD data on their own can clearly be beneficial to the analyses and subsequent forecasts of the moisture field. This result suggests that the potential impact of precipitation observations is overshadowed by the influence of other high-quality humidity observations, in particular radiosondes. It also confirms that the assimilation of precipitation observations has the ability to improve the quality of moisture analyses and forecasts in data sparse regions. Finally, the limitations inherent in the current assimilation of precipitation data, their implications for the future and possible ways of improvement are discussed.

# 1 Introduction

During the last decade, the data assimilation community has attempted to find the optimal way to extract information from observations that are affected by clouds and/or precipitation, with the hope that this could help improve operational weather analyses and forecasts. A large amount of such observations is already available from various spaceborne platforms such as SSM/I, SSMIS, TRMM, AQUA, and MODIS (see Appendix 1 for abbreviations related to satellite and institutions). More is expected from the recently launched CloudSAT and from future missions such as GPM (2010-2012). All these observations consist of either direct measurements of multi-frequency radiances (mainly in the microwave and infrared bands), radar reflectivities or lidar backscattering cross-sections, or of retrieved quantities (e.g. optical depth, rain rates). Ground-based measurements are also available from national radar networks (e.g. Europe, United States) and rain gauges, as well as from a few heavily instrumented experimental sites throughout the world, such as those of the Atmospheric Radiation Measurement Program (ARM; Stokes and Schwartz 1994) for instance. Data from the latter have turned out to be very useful for research developments (e.g. Lopez *et al.* 2006) but offer very little interest for operational global assimilation due to their obviously limited spatial coverage.

Several approaches have been tested to account for cloud and precipitation observations in numerical weather prediction (NWP): nudging (Macpherson 2001), diabatic initialization (Ducrocq *et al.* 2002), variational methods (e.g. 4D-Var) and Ensemble Kalmán Filter. Although the variational approach was successfully implemented by many operational weather services to assimilate non-cloudy data more than a decade ago, its underlying requirements of linearity and Gaussian model and observation error distributions have made its application to measurements in cloudy and precipitation regions much more difficult. Moist processes must be involved in the definition of the observation operator that converts the model control variables (typically temperature, moisture, wind and surface pressure) into equivalent observed quantities (e.g. precipitation, radiances, reflectivities). These processes are naturally nonlinear (e.g. saturation, convective regimes) and a special treatment has to be applied to avoid discontinuities (thresholds, switches) (Zupanski 1993; Vukićević and Errico 1993; Zou 1997; Vukićević and Bao 1998); otherwise the result of the variational analysis is not optimal or even worse the minimization of the cost function can fail. In other words, to develop new physical parameterizations of moist processes that can be utilized in a variational data assimilation system, one needs to find the best compromise between realism, linearity and computational efficiency (e.g. Mahfouf 1999; Janisková *et al.* 1999). A recent review of these important issues, many of which remain unsolved, can be found in Lopez (2006) for instance.

Early attempts to assimilate satellite rain rates in variational systems were conducted by Treadon 1997, Hou *et al.* (2001), Hou *et al.* (2004), Peng and Zou (2002) , Marécal and Mahfouf (2002, 2003). Slight global improvements of analyses and forecasts could be obtained in terms not only of moisture fields but also in terms of the dynamics. Rain-rate assimilation even became operational in 3D-Var at NCEP (Treadon *et al.* 2002) and in 4D-Var at JMA (Tsuyuki *et al.* 2002). At ECMWF, SSM/I rain-affected 19 GHz and 22 GHz brightness temperatures have been operationally assimilated since June 2005 (Bauer *et al.* 2006a, 2006b) using the two-step "1D+4D-Var" technique originally proposed by Marécal and Mahfouf (2003).

Taking advantage of the new framework developed at ECMWF for the assimilation of SSM/I rain-affected brightness temperatures, the present work investigates the feasibility and the impact of the "1D+4D-Var" assimilation of NCEP Stage IV hourly surface precipitation data (Baldwin and Mitchell 1996; Lin and Mitchell 2005), which combine measurements from the network of ground-based radars (NEXRAD) and rain gauges over the continental United States (US). In the following, the NCEP Stage IV hourly precipitation observations shall be referred to as "NEXRAD observations" for the sake of brevity.

Section 2.1 provides a short description of the "1D+4D-Var" assimilation method. The NEXRAD observations to be assimilated and their associated error statistics are detailed in section 3. The results of the assimilation experiments are presented in section 4 while the main issues they raise are discussed in section 5. Section 6 summarizes the results and issues found in this study and the implications for the assimilation of precipitation observations in 4D-Var.

# 2 "1D+4D-Var"

## 2.1 Method

The so-called "1D+4D-Var" was first introduced by Marécal and Mahfouf (2003) to assimilate surface rain rate retrievals from SSM/I and TRMM Microwave Imager (TMI). The method was then extended to be directly applied to SSM/I microwave brightness temperatures (MW TBs) and became operational at ECMWF in June 2005 (Bauer *et al.* 2006a, 2006b). First, the raw measurements are used in a 1D-Var procedure to produce increments of specific humidity that are vertically integrated and added to the model background to produce Total Column Water Vapour (TCWV) retrievals. These pseudo-observations in rainy regions are then assimilated into ECMWF's 4D-Var system (Courtier *et al.* 1994) together with millions of other clear-sky observations . In the present study, NEXRAD precipitation estimates are fed into the 1D-Var instead of SSM/I MW TBs. From a technical point of view, the same stream of code could be used to assimilate both types of data, which made the implementation easier. It should be underlined that NEXRAD observations provide a complementary source of information over land since SSM/I MW TBs are currently assimilated over ocean only because of the unsolved issue of surface emissivity modelling over land.

As a reminder, the 4D-Var method searches for the model state vector at the initial time of a given time window, $\mathbf{x}_0$, that minimizes the following cost function

$$J(\mathbf{x}_0) = \underbrace{\frac{1}{2}(\mathbf{x}_0 - \mathbf{x}_0^b)^T \mathbf{B}^{-1}(\mathbf{x}_0 - \mathbf{x}_0^b)}_{J_b} + \underbrace{\frac{1}{2}\sum_t (H_t(\mathbf{x}_0) - \mathbf{y}_t)^T \mathbf{R}_t^{-1}(H_t(\mathbf{x}_0) - \mathbf{y}_t)}_{J_o} \quad (1)$$

where subscript $t$ denotes the model timestep and $\mathbf{x}_0^b$ is the background model state at the initial time. In 4D-Var, $\mathbf{x}_0$ consists of temperature, humidity, vorticity, divergence and surface pressure. $H_t$ is the nonlinear observation operator that converts the initial model state into observed equivalents at time $t$ for comparison with the corresponding observations $\mathbf{y}_t$. $\mathbf{R}$ is the error covariance matrix of the observations which may be

time-dependent. Matrix **B** contains the background error covariances for each model variables and is based on a wavelet formulation (Fisher 2004) to introduce regime-dependent error statistics. The result of 4D-Var is therefore the optimal combination of the background information ($J_b$) with information coming from the available observations ($J_o$), weighted by the inverse of their respective error covariances. In the case of 1D-Var, the problem is solved in a similar way, except that only the vertical dimension is considered and that only temperature and specific humidity are included in $\mathbf{x}_0$.

### 2.2 Linearized physics

One important component of the assimilation system is the linearized physical package that is used in both 1D-Var and 4D-Var minimizations. Indeed, previous studies have demonstrated that the inclusion of linearized simplified physical parameterizations in the 4D-Var minimizations improves the underlying tangent-linear assumption and thereby the 4D-Var analyses and subsequent forecasts (e.g. Tsuyuki 1997; Janisková *et al.* 1999). In 1D-Var, moist physical schemes are necessary to convert the model state into precipitation rates that can be compared to NEXRAD observations. The 1D-Var part of the assimilation utilizes the two new linearized parameterizations of large-scale condensation (Tompkins and Janisková 2004) and convection (Lopez and Moreau 2005). In 4D-Var, the operational linearized simplified schemes (Mahfouf 1999; Janisková *et al.* 2002) are activated to describe radiation, vertical diffusion, gravity wave drag, convective and large-scale moist processes. This combination of physical parameterizations is the same as in current operational "1D+4D-Var" applied to SSM/I rain-affected radiances. However, in the coming months, the more detailed moist physical simplified schemes of Tompkins and Janisková (2004) and Lopez and Moreau (2005) are meant to become operational in 4D-Var minimizations as well, which will ensure more consistency with 1D-Var.

## 3 Observations

### 3.1 NCEP Stage IV precipitation dataset

The NCEP Stage IV precipitation dataset contains precipitation analyses obtained from approximately 150 high-resolution Doppler NEXt-generation RADars (NEXRAD) and about 5,500 hourly rain-gauge reports over the continental USA (Baldwin and Mitchell 1996; Lin and Mitchell 2005). Technically, the NEXRAD instrument corresponds to the so-called WSR-88D (Weather Surveillance Radar, 1988, Doppler) (Fulton *et al.* 1998). In this study, only main land US Stage IV data (excluding Alaska) have been used. The original precipitation accumulations were available on a 4-km resolution polar-stereographic grid and were averaged onto the ECMWF model's T511 Gaussian grid (≈40 km) before being assimilated. Each NCEP Stage IV precipitation analysis is started at 35 min after the top of each hour and is then progressively updated over several hours with new data coming from each of the twelve US regional centres. A first inflow of automatically generated analyses is available within a few hours after the accumulation time, while a second inflow of updated manually-quality-controlled analyses becomes available later (with a delay of up to 12 hours). In this work, the "1D+4D-Var" experiments are based on manually quality controlled hourly precipitation accumulations that were obtained from the archive at JOSS/UCAR (website: *http://www.joss.ucar.edu/codiac/*).

### 3.2 Change of variable and screening

To alleviate the problem of non-normal distributions often encountered when working with precipitation data (Errico *et al.* 2000), the decimal logarithm of the NEXRAD precipitation ($log(RR)$ hereafter) is used in 1D-Var.

Such conversion was already successfully applied by Hou *et al.* (2004), for instance. Besides, since the 1D-Var can only work when there is at least a small amount of precipitation in the model background (otherwise the rainfall sensitivities are equal to zero), only points where the background hourly precipitation rate is higher or equal to 0.1 mm $h^{-1}$ are used in the 1D-Var. To avoid the possible development of a dry bias after 1D-Var due to this one-sided screening, points where the observed rainfall value is lower than 0.1 mm $h^{-1}$ are also rejected prior to 1D-Var. Eventually, the total number of active NEXRAD observations in 4D-Var is approximately 1200 for each 12-hour assimilation cycle. Because of the chosen screening, this number depends at each cycle on the total area of the US affected by precipitation higher or equal to 0.1 mm $h^{-1}$ both in the model and in the observations.

### 3.3 Errors

For the purpose of filling matrix **R** that describes the error statistics of the observation operator $H_t$ in 1D-Var, the relative error of the NEXRAD hourly precipitation rates, $\varepsilon$, is set to

$$\varepsilon \quad = \quad 0.2 + 0.3 \, \frac{\sigma_{orog}}{1200} \tag{2}$$

where $\sigma_{orog}$ is the standard deviation of the subgrid scale orography used in the model (in metres). This formulation is meant to increase the observation error over mountainous terrain to account for the lower representativeness of precipitation measurements from both radars and rain gauges. Practically, $\varepsilon$ varies between 20% over flat terrain and about 40% over the Rocky Mountains. The occurrence of surface snowfall and high surface wind speed are also known to increase the errors in rain gauge measurements, but their effects have not disregarded in the late-spring situations considered in this study. The selected formulation for $\varepsilon$ is rather arbitrary given the current uncertainties both in NEXRAD observations and in the moist physical parameterizations (involved in the observation operator). However, preliminary tests have shown that the results of "1D+4D-Var" experiments with NEXRAD data are not very sensitive to the coefficients specified in Eq. (2). This equation yields the error standard deviation of the decimal logarithm of the NEXRAD rain rates

$$\sigma_{logRR} \quad = \quad \sqrt{\log(1+\varepsilon^2)} \tag{3}$$

By construction, the 1D-Var framework does not permit the inclusion of horizontal correlations of NEXRAD observation representativeness errors, and for simplicity TCWV pseudo-observation errors that are output from 1D-Var and input to 4D-Var are supposed to be spatially uncorrelated as well. The specification of the standard deviation of TCWV pseudo-observation errors, $\sigma_{TCWV}$ (in kg $m^{-2}$), is the one used in the operational "1D+4D-Var" assimilation of rain-affected SSM/I observations (model cycle 29r2), that is

$$\sigma_{TCWV} \quad = \quad 0.872 + 1.139\left(\frac{TCWV}{16}\right) - 0.155\left(\frac{TCWV}{16}\right)^2 \tag{4}$$

This formulation was obtained through statistical regression on 1D-Var outputs. In theory, errors in $H_t$ might be correlated in the horizontal since NEXRAD observations are partially based on radar measurements and because the forecast model is part of the observation operator. This issue is beyond the scope of the present feasibility study but will deserve some attention in the near future. Another limitation of the 1D-Var framework lies in the fact that hourly NEXRAD rain accumulations are compared to model precipitation amounts that are obtained over a single time step of 15 min. However, preliminary experimentation showed a marginal impact from assimilating accumulations that had been linearly interpolated in time to match the 15 min time step instead of hourly accumulations (not shown). The time mismatch has therefore been disregarded in this work. In fact, the actual assimilation of accumulated precipitation will only become possible with a direct 4D-Var approach.

# 4 Experiments

## 4.1 Set-up

Two "1D+4D-Var" experiments have been run between 0000 UTC 20 May 2005 and 0000 UTC 20 June 2005 to assess the impact of the assimilation of hourly NEXRAD observations on both analyses and subsequent forecasts. It should be underlined that spring precipitation over the US is predominantly associated with convective situations, which are known to be more problematic for weather forecasting systems than typical winter conditions and therefore more interesting to study. The control experiment (CTRL hereafter) is a 4D-Var assimilation of all observations that are routinely treated in operations at ECMWF. These include SSM/I rain-affected radiances over ocean that have been assimilated through "1D+4D-Var" since June 2005. In the second experiment (NEW hereafter), NEXRAD observations have been used in addition to all other observations. Figure 1 provides an example of the spatial coverage of all types of observations affected by moisture over the US for a single 12-hour cycle of 4D-Var, at 0000 UTC 20 May 2005. These include conventional surface humidity measurements (SYNOP) and radiosoundings (TEMP), radiances from various polar-orbiting satellites (NOAA HIRS and AMSU-B, AIRS, DMSP SSM/I) and two geostationary satellites (GOES-10 and 12). Abbreviations are detailed in Appendix 1. The NEXRAD rain observations that have been assimilated in "1D+4D-Var" are shown in Fig. 1g and were mainly concentrated in the eastern part of the US on the selected date. It should be noted that the permanent absence of 2-meter humidity SYNOP observations over the western US can be explained by their blacklisting due to excessive orography discrepancies between model and stations over the Rocky Mountains or by their rejection due to too large background departures (east of the Rocky Mountains). In all experiments, 60 vertical levels have been used and the horizontal spectral resolution in the forecasts and in the 4D-Var trajectory computations (outer loops) has been set to T511 (≈40 km) while the first and second iterative minimizations of 4D-Var (inner loops) have been run at T95 (≈210 km) and T159 (≈120 km) respectively (Andersson *et al.* 2005). Except for the changes of linearized moist physics described in section 2.2, the code used here is based on cycle 29r2 (operational from June 2005) of the ECMWF model. Finally, it should be noted that some of the statistics presented below have been calculated over periods of time shorter than the actual length of the experiments to limit computational cost and storage requirements, provided the sample size was deemed large enough.

## 4.2 Results

### *4.2.1 1D-Var*

First, the behaviour of the 1D-Var retrieval applied to NEXRAD observations to generate pseudo-observations of TCWV is examined. Figure 2 illustrates the relationship between the 1D-Var TCWV increments and the observation minus background $log(RR)$ departures. The statistics are based on 32450 points over 27 assimilation cycles. As expected from physical common sense, positive/negative $log(RR)$ departures (i.e. too little/much rain in the model) usually lead to a moistening/drying of the model state after 1D-Var. However, there are few points where an opposite link is found, which indicates the presence of some nonlinearities associated with moist processes, but this does not seem to hamper the convergence of the subsequent 4D-Var minimizations. In future experimentation, these points should be rejected before 4D-Var.

Figure 3 shows probability distribution functions (PDFs) of background and 1D-Var analysis $log(RR)$ departures, TCWV increments and background $log(RR)$. The PDF of observation minus background departures (Fig. 3a) exhibits a Gaussian shape and the rather small negative mean departure ($-0.171$) indicates that the model tends to have slightly too much precipitation on average compared to NEXRAD. Since this bias is quite

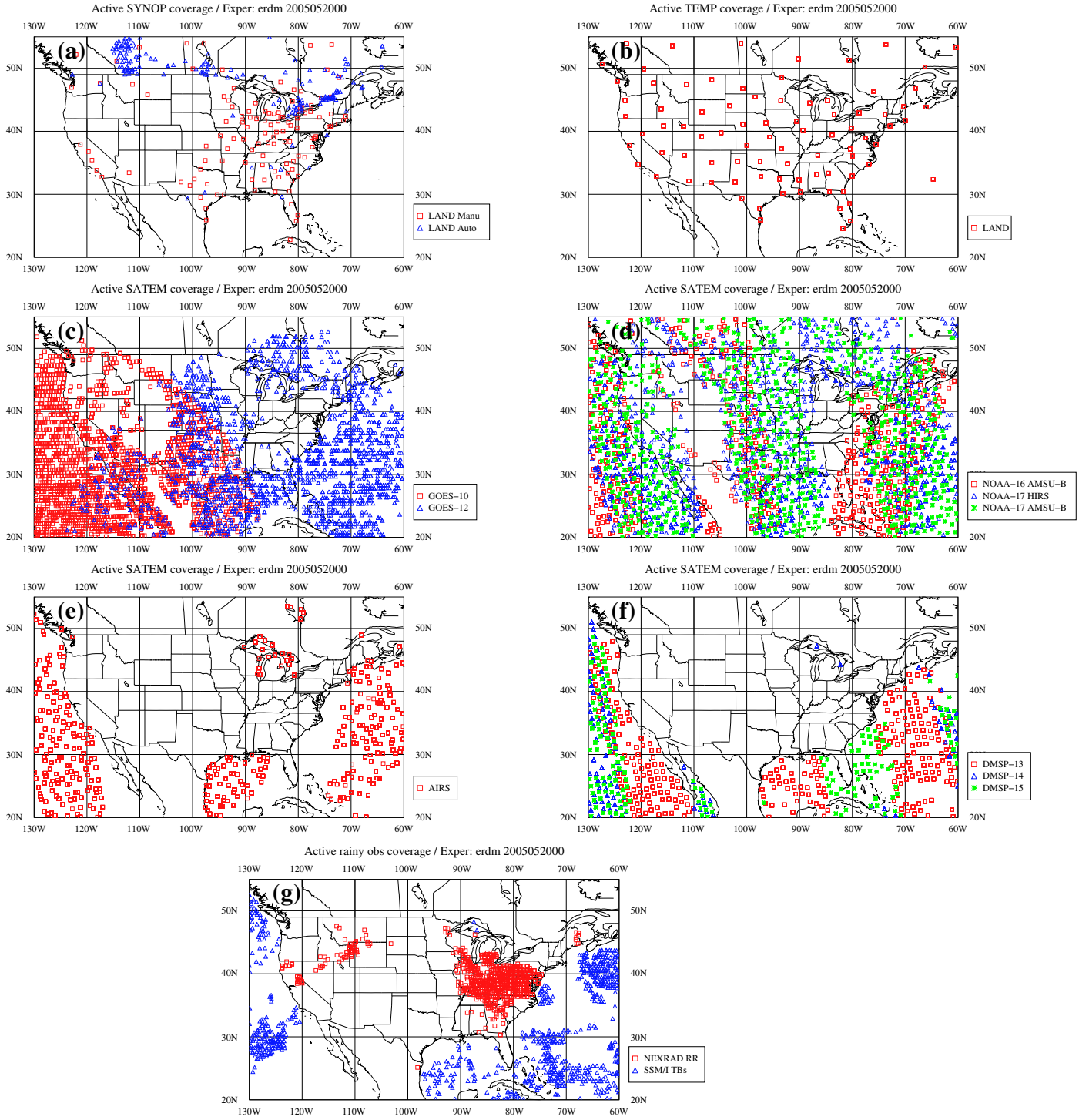


FIGURE 1: Example of spatial coverage of moisture-sensitive observations assimilated over the US in a single 12-hour cycle of 4D-Var at 0000 UTC 20 May 2005: (a) SYNOP (manual and automatic), (b) radiosoundings, (c) GOES (water vapour channel), (d) NOAA (HIRS and AMSU-B), (e) AIRS, (f) DMSP SSM/I clear-sky TBs and (g) DMSP SSM/I rain-affected TBs (ocean) and the new NEXRAD observations (land). Colour symbols correspond to various observation types, satellites or instruments, as indicated in the legend of each plot.

small, no *a priori* rain bias correction has been applied. After 1D-Var (Fig. 3b), the PDF of analysis departures becomes much more narrow, which suggests that the 1D-Var was able to produce proper increments to adjust the model precipitation towards NEXRAD observations. The mean departure is also substantially reduced in the 1D-Var analysis (0.004) which proves that the 1D-Var also removed the slight bias seen in the background precipitation. Only a modest negative dry bias ($-0.239$ kg m$^{-2}$) can be found on average in the PDF of the 1D-Var TCWV increments (Fig. 3c) and the shape of the distribution is again not too far from being Gaussian, which is a nice feature. Finally, Fig. 3d shows that the logarithmic change of variable applied to precipitation helps to reduce the skewness of the original PDF of background precipitation (not shown). In view of these statistics, it can be concluded that the behaviour of the 1D-Var step is satisfactory, with no systematic large bias either in the input background rain or in the output TCWV retrievals and with good convergence towards observations.

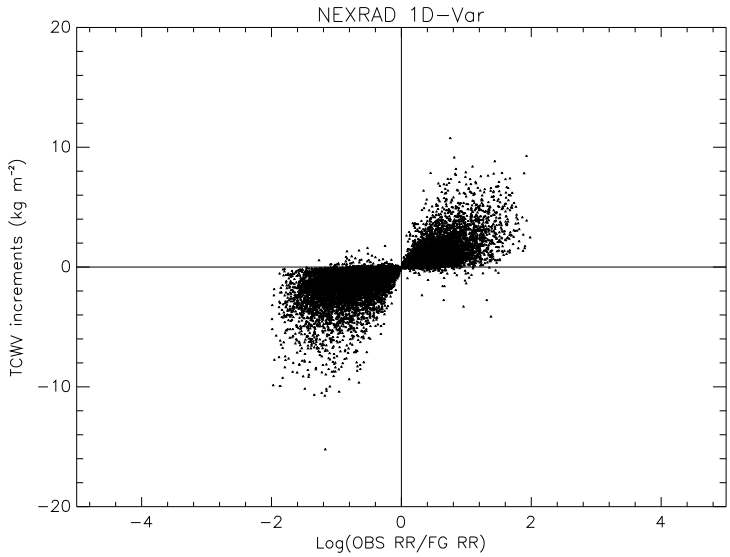


FIGURE 2: Scatter plot of TCWV increments from 1D-Var with NEXRAD observations as a function of observation minus background $log(RR)$ departures, over the period 0000 UTC 20 May 2005 to 1200 UTC 1 June 2005. Departures in $log(RR)$ are unitless and TCWV increments are in kg m$^{-2}$.

### *4.2.2 4D-Var*

**Analyses and forecasts of standard fields**

The mean impact of the assimilation of NEXRAD observations on 4D-Var TCWV analyses is displayed in Fig. 4. There is a clear moistening (up to 1.5 kg m$^{-2}$) over the central US, east of the Rocky Mountains, and a drying of similar magnitude but less widespread over northwestern Florida, two regions where most of the US rainfall occurs during the period of the experiment (see paragraph about precipitation). A drying is also found over the north of Mexico. Otherwise, the mean impact on the temperature analysis is very limited (even over the US) and is negligible for wind, geopotential and surface pressure (not shown). This lack of interaction of moisture changes with the dynamics and temperature in the analysis will be discussed in section 5.

In subsequent forecasts, the signal that was found in the analyzed moisture field in Fig. 4 survives for one day with a reduced amplitude though and later evolves into more widespread patterns (not shown). The fast decaying of the moistening associated with NEXRAD data could be due to the fact that the extra moisture is rained out during the first hours of the forecast. To determine whether the modifications in the humidity analysis

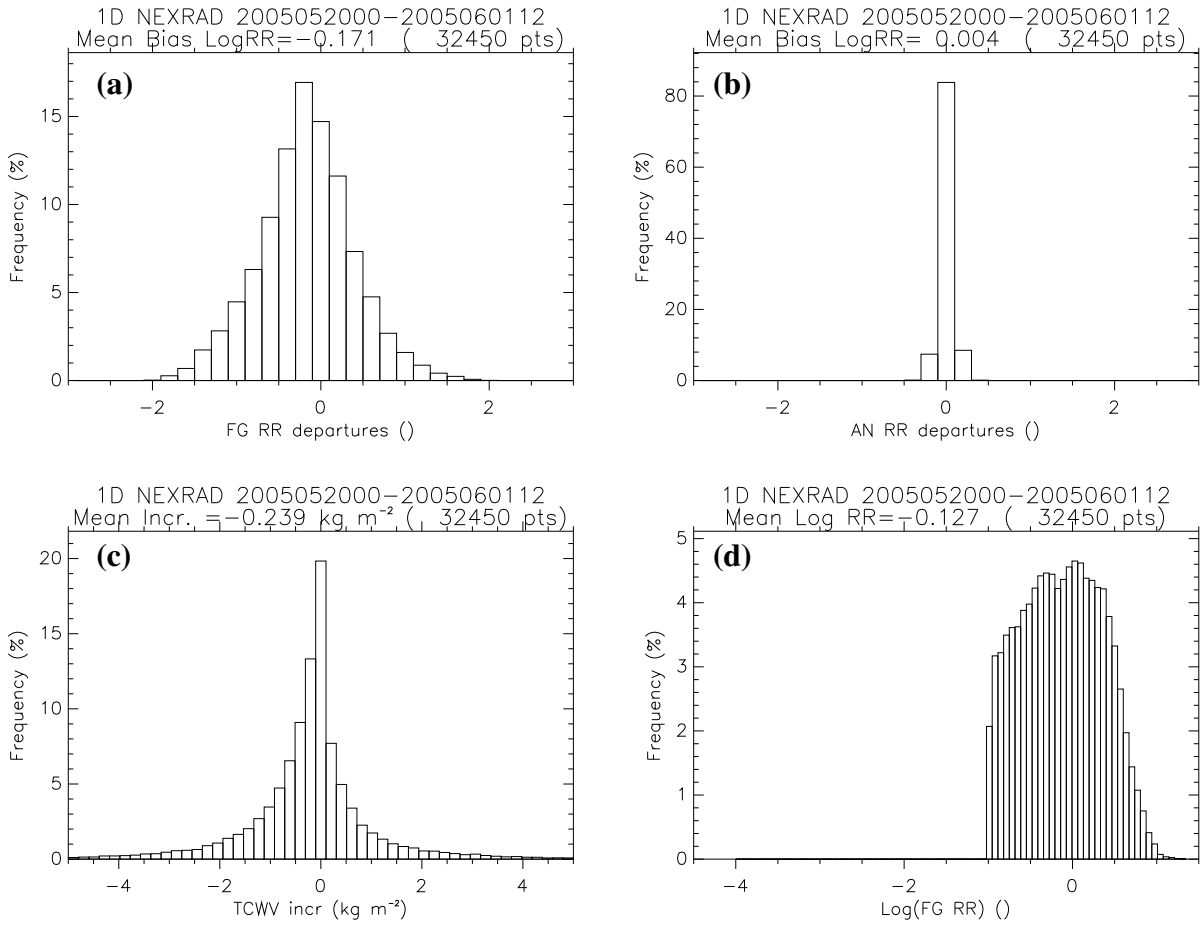


FIGURE 3: PDFs of 1D-Var with NEXRAD rain observations computed from 0000 UTC 20 May 2005 to 1200 UTC 1 June 2005: (a) observation minus background $log(RR)$ departures, (b) observation minus 1D-Var analysis $log(RR)$ departures, (c) 1D-Var TCWV increments and (d) background $log(RR)$. In (a) and (b), $log(RR)$ departures are unitless, while TCWV increments in (c) are in kg m$^{-2}$ and $log(RR)$ in (d) is in log[mm h$^{-1}$]. Frequencies (y-axis) are in %. Mean values are given in the title of each plot.

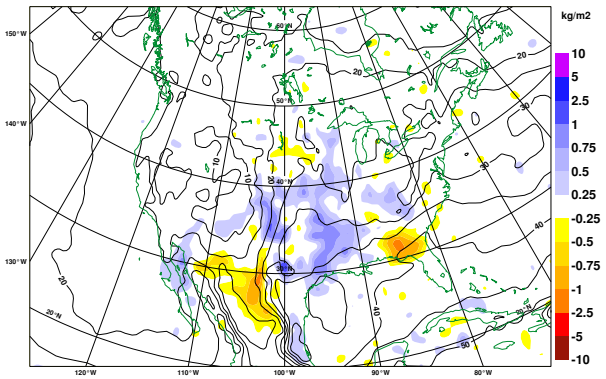


FIGURE 4: Map of NEW−CTRL mean differences in 4D-Var TCWV analysis at 0000 UTC (color shading; in kg m$^{-2}$; see text for detail on experiments). Isolines show the corresponding mean analyzed TCWV from experiment CTRL (contour interval: 5 kg m$^{-2}$).

could still impact on other fields in the forecasts, traditional scores have been computed from CTRL and NEW for geopotential, temperature and wind for various geographical domains and for forecast ranges between one and ten days. Both root-mean-square forecast error ($RMSFE$) and forecast anomaly correlation have been studied. The mean impact of the assimilation of NEXRAD observations on both scores turns out to be either neutral (usually) or slightly positive for some specific parameters, levels and forecast ranges. A sample of the most noticeable features is illustrated in Fig. 5 that displays the normalized NEW−CTRL changes in $RMSFE$ for geopotential height and for selected levels and geographical domains. The $RMSFE$ difference is normalized by the mean of the $RMSFE$ from the two experiments and error bars for a 90% two-sided confidence level (t-test) are also shown. A positive (resp. negative) value indicates a degradation (resp. an improvement) of the forecast. The overall impact from the NEXRAD observations is rather neutral over the Northern Hemisphere (Fig. 5a). Over North America (Fig. 5b), the 1000-hPa geopotential $RMSFE$ is significantly improved by up to 2.5% until day 3. Over the North Atlantic (Fig. 5c), there is a clear improvement of 200-hPa geopotential by about 5% around days 3-4, which could result from the downstream propagation of the positive impact seen over North America at shorter forecast ranges. The same mechanism could explain the improvement detected at days 7-8 over Europe (Fig. 5d). Similar improvements are found for the temperature and wind fields (not shown) for the same levels and domains selected in Fig. 5. For other levels and domains, the impact of the NEXRAD rain data is neutral (not shown). The overall modest influence on analyses and forecasts can be explained by the limited spatial coverage (US only) and the relatively small number of NEXRAD observations ( 1200 per cycle) compared to the hundred thousands of worldwide observations already available in CTRL. The potential impact of NEXRAD observations when they are assimilated on their own will be studied in section 5. The validation of analyses and forecasts against radiosondes only indicated a marginal improvement on average in NEW compared to CTRL (not shown).

**Precipitation forecasts**

More interestingly, the impact of NEXRAD data on precipitation scores has been assessed by comparing precipitation forecasts from CTRL and NEW to the NEXRAD observations over the US. It should be recognized here that, because some of them are assimilated through "1D+4D-Var", NEXRAD measurements cannot be considered as truly independent data for forecast ranges up to 9 hours. All statistics in this section have been calculated for the entire month of the experiments. Maps of mean precipitation accumulations from NEXRAD, differences CTRL−NEXRAD and NEW−CTRL are shown in Fig. 6 and Fig. 7 for 0-6h, 6-12h, 12-18h and 18-24h forecasts started at 0000 UTC. For convenience, the local-time slots corresponding to these forecast ranges will be referred to as evening, night, morning and afternoon, respectively. Figure 9 displays combined statistics in time and space: the NEXRAD mean 6-hour precipitation, the corresponding experiment minus NEXRAD mean bias, the time-mean root-mean-square (RMS) experiment minus NEXRAD difference and the time-mean correlation between experiment and NEXRAD. Similar statistics are plotted in Fig. 10 for 12-hour intervals up to five days. Curves are shown for three geographical domains defined in Fig. 8. Subdomains CentUS and SEasUS were chosen because they encompass most of the rainfall falling over the US during the selected month (Fig. 6a,d and Fig. 7a,d) and because they are characterized by quite different observed diurnal cycles of precipitation. Indeed over CentUS (resp. SEasUS), rainfall is maximum during the evening and night (resp. afternoon), and is minimum in the morning (resp. night) (Fig. 9a).

First, the quality of the 6-hour accumulated precipitation forecasted from CTRL is assessed over a month by focusing on panels (a),(b),(d) and (e) of Fig. 6 and Fig. 7 as well as on the solid curves in Fig. 9a,b. Over CentUS, observed precipitation is underestimated by more than 1 mm day$^{-1}$ on average (roughly 33%) in the evening and during the night, but is overestimated by a similar percentage in the morning and the afternoon. Over SEasUS, the model lacks roughly 15% of the NEXRAD precipitation amount in the afternoon and in the evening. About the right amount is produced during the night, but morning rainfall is heavily overestimated over most of the domain, by more than 2 mm day$^{-1}$ on average (i.e. by 90%). Over the entire US domain,

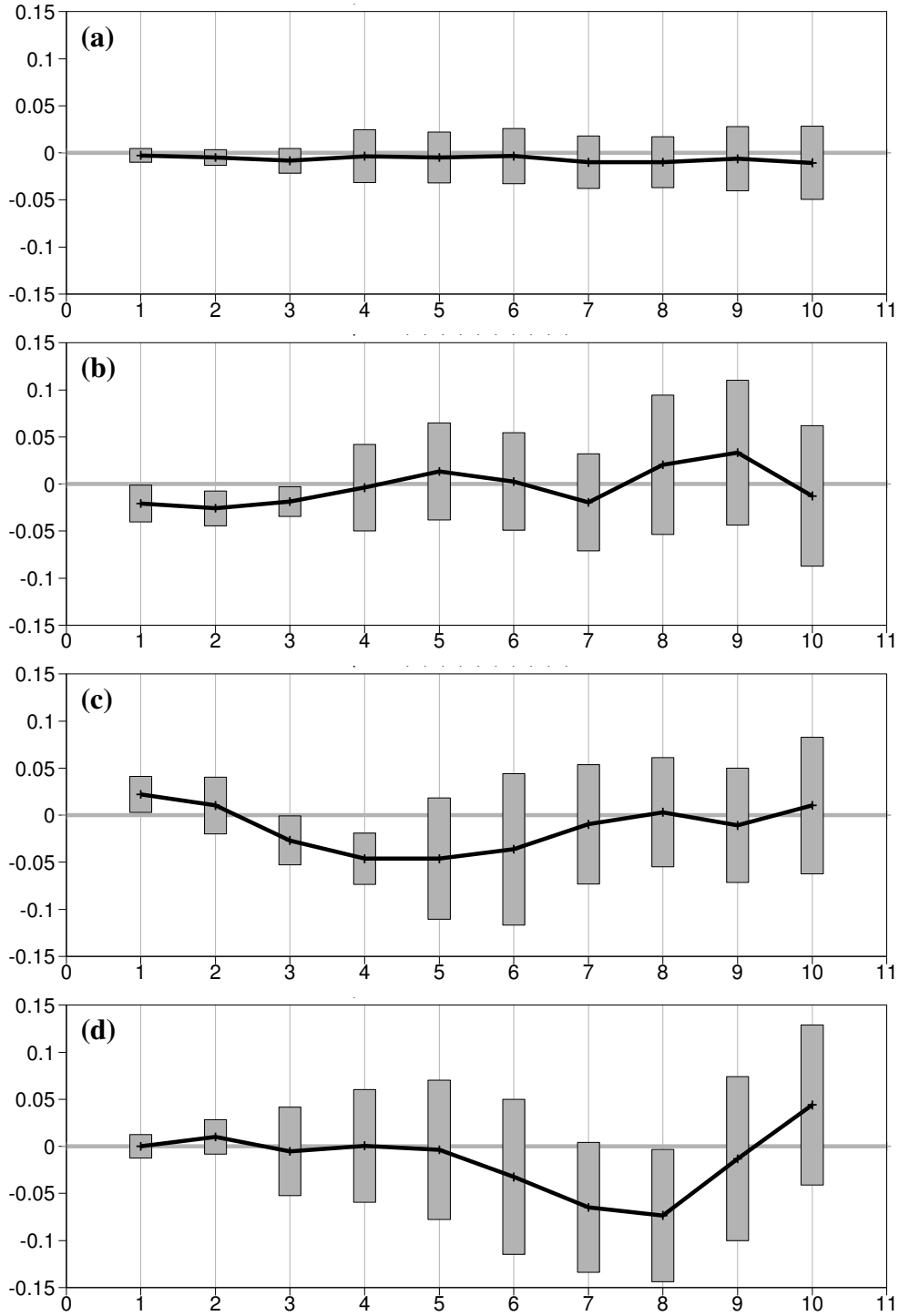


FIGURE 5: Normalized changes in root-mean-square forecast error due to the assimilation of NEXRAD observations in terms of geopotential height at level (a) 1000-hPa in the Northern Hemisphere, (b) 1000-hPa over North America, (c) 200-hPa over the North Atlantic and (d) 850-hPa over Europe. Forecast ranges (x-axis) are in days and *RMSFE* changes (y-axis) are unitless. Scores have been computed over twenty-one 4D-Var cycles between 0000 UTC 20 May 2005 and 0000 UTC 9 June 2005 against own analyses (21 cases). Error bars (grey boxes) for a 90% two-sided confidence level (t-test) are also plotted.

the dominant contributions from the two previous domains result in an overall 15-25% underestimation in the evening and at night and in a strong overestimation (60%) in the morning, much slighter (10%) in the afternoon. Statistics computed for 12-hour intervals over five days (Fig. 10b) indicate that the overestimation of precipitation during daytime (morning and afternoon) over SEasUS remains almost unchanged when forecast range is increased. The excessive amount of rainfall simulated in the morning over SEasUS suggests that convection is triggered several hours too early in this region. On the other hand, the forecasts at longer ranges seem to recover from the nighttime rainfall underestimation that was found over CentUS in Fig. 9b, which points to the existence a local spin-up problem. At the same time, the daytime precipitation over CentUS remains overestimated at all ranges. Eventually, the combination of panels (a) and (b) of Fig. 10 shows that the diurnal cycle of precipitation over CentUS is far too weak in the model compared to NEXRAD observations. Cheinet *et al.* (2005) have shown that cycle 28r1 (operational from March 2004) of the ECMWF model had difficulties to forecast the diurnal cycle of precipitation correctly over the US Southern Great Plains. This deficiency was attributed to an imperfect representation of the eastward propagation of upper-tropospheric disturbances away from the Rocky Mountains and of their interaction through boundary layer processes and convection with the moist low-level jet originating from the Gulf of Mexico. The more recent model cycle used in this study still suffers from this deficiency.

As far as the differences between NEW and CTRL are concerned, Fig. 9b indicates that the mean error in the model precipitation is not greatly modified by the additional NEXRAD observations, except for a further reduction of rainfall over SEasUS for the 0-6h range. On the other hand, the RMS model error is reduced by 5 to 10% for forecast ranges shorter than 12 hours and for all domains (Fig. 9c). Beyond 12 hours, the RMS is still reduced but by a smaller amount. Consistently with the RMS results, the correlation coefficient between the model and NEXRAD is increased by roughly 0.1 for forecast ranges up to 12 hours when NEXRAD observations are assimilated, but again this improvement almost vanishes beyond 12 hours. The lower mean RMS error and the higher mean correlation in NEW compared to CTRL indicates that the spatial variability of the error is reduced and that precipitation patterns in the model are in better agreement with the observations. The point-by-point comparison of panels (b) against (c), and panels (e) against (f) of Fig. 6 and Fig. 7 also demonstrates that the assimilation of NEXRAD observations yields changes in the precipitation field that are often opposite to the CTRL errors, therefore going in the correct direction. This is particularly true for the 0-6h forecast in Fig. 6b,c. Figure 10b-d confirms that the positive impact of NEXRAD observations is confined to short forecast ranges. Of course, one should remember that for forecast ranges up to 12 hours some of the NEXRAD observations used in the validation process were assimilated in the 4D-Var assimilation window (21:00-09:00) and thus cannot be considered as fully independent data. This could account for the larger positive impact seen in NEW at short ranges. Another possible explanation is that the impact of the moisture increments associated with NEXRAD observations can be quickly lost during the forecasts due to some shortcomings of the "1D+4D-Var" approach (see section 5).

Traditional scores of model precipitation against NEXRAD observations have also been computed for experiments CTRL and NEW and for different rainfall thresholds. They are displayed in Fig. 11 for the 12-h forecast (started at 0000 UTC) and for the entire US domain. These scores consist of the Frequency Bias ($FB$), the Equitable Threat Score ($ETS$), the Probability Of Detection ($POD$) and the False Alarm Rate ($FAR$) (see Appendix 2 for a reminder of their definition). For this specific forecast range (12h), $FB$ remains close to unity for rain thresholds below 10 mm day$^{-1}$ and decreases with threshold value above. This indicates that the model tends to underpredict the occurrence of heavy rain events. This tendency is slightly enhanced in experiment NEW. On the other hand, $ETS$ is increased in NEW compared to CTRL, which corresponds to an improvement. $POD$ is slightly improved for thresholds below 10 mm day$^{-1}$ and unchanged above, while $FAR$ is clearly reduced for heavier rain rates. The impact of NEXRAD data remains slightly positive up to 72 hours, then vanishes and becomes slightly negative beyond 84 hours (not shown). From all these validations performed on precipitation one can conclude that the impact of the "1D+4D-Var" assimilation of NEXRAD rain rates in the forecasts is

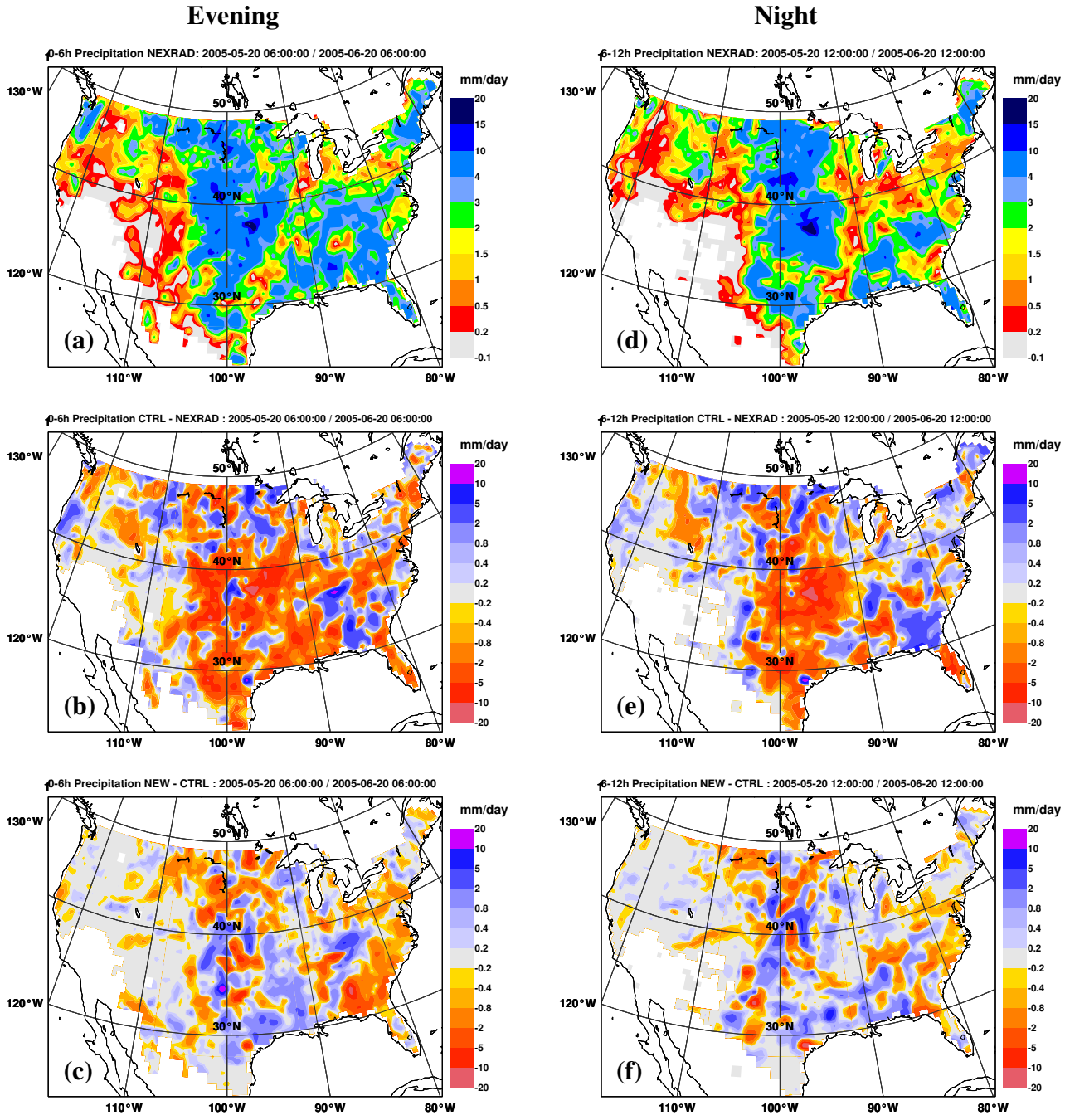


FIGURE 6: Maps of mean precipitation accumulations over the US for forecast ranges 0-6h (left column) and 6-12h (right column): (a,d) NEXRAD observations, (b,e) difference CTRL−NEXRAD and (c,f) difference NEW−CTRL. All fields are expressed in mm day$^{-1}$.

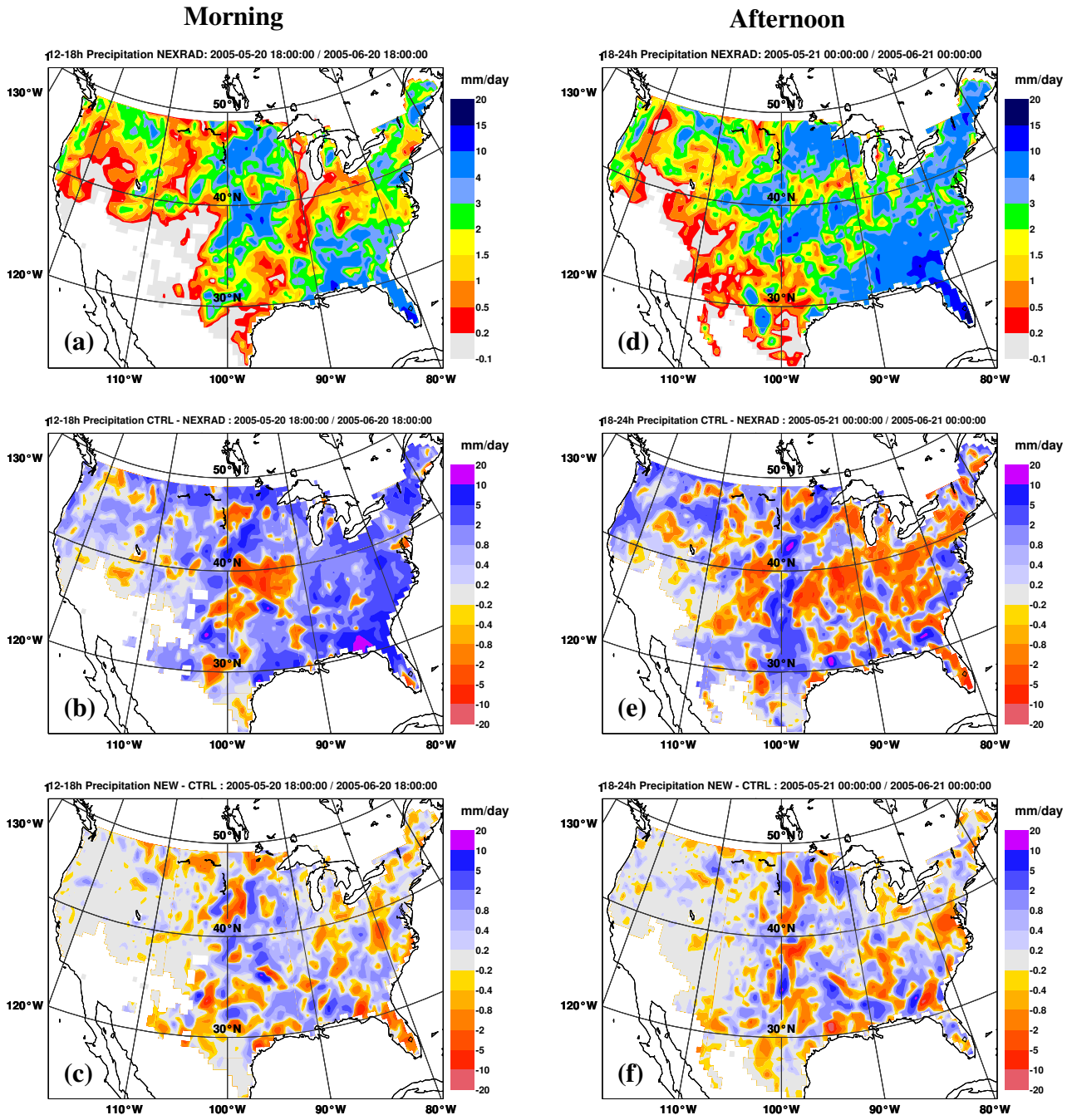


FIGURE 7: Same as in Fig. 6 but for forecast ranges 12-18h (left column) and 18-24h (right column).

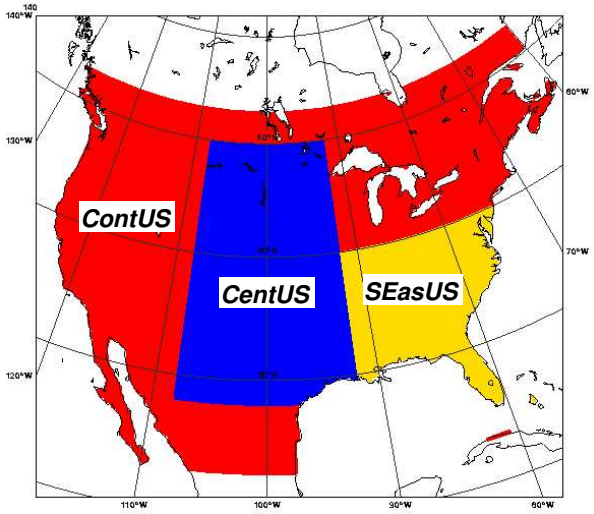


FIGURE 8: The three geographical domains used in the computations of precipitation statistics: ContUS = entire US main land plus northern Mexico and southern Canada (red), CentUS = central US (blue) and SEasUS = southeastern US (yellow). ContUS encompasses CentUS and SEasUS.

positive only for the short ranges (up to 12 hours) and rather neutral beyond.

**Radiation**

The impact of NEXRAD assimilation on clouds has also been checked by computing statistics of background departures w.r.t. HIRS cloudy TBs over the US. HIRS infrared channel 8 (11.11 $\mu$m) has been selected because these data are currently not assimilated in the 4D-Var wherever clouds are detected. Figure 12 displays a frequency histogram of the corresponding background departures built from 505797 cloudy locations in experiment CTRL between 25 May and 3 June 2005. The distribution exhibits a Gaussian shape with a mean bias equal to $-2.98$ K and a standard deviation of 13.21 K. For experiment NEW, the histogram looks similar (not shown), but the mean becomes $-2.91$ K and the standard deviation is reduced to 13.11 K. These changes indicate a small but overall improvement of the fit between the model background and HIRS cloudy infrared radiances.

# 5 Discussion

In section 4, it was found that assimilating hourly NEXRAD rain observations through "1D+4D-Var" modified the moisture analyses but did not affect very much the mass and dynamical fields. Furthermore, the improvement of forecasted precipitation over the US was limited to the first twelve hours of the model integration. This rather modest impact of NEXRAD data is likely due to the large amount of observations that are already routinely available over North America, which includes high-quality radiosoundings and surface observations and satellite data with good spatial coverage and temporal sampling. In particular, NEXRAD observations are directly competing with all other moisture-dependent observations, as illustrated in Fig. 1. In order to verify that the assimilation of NEXRAD observations could have a positive impact on their own, a "1D+4D-Var" experiment has been run in which all observation types directly affected by moisture as shown in Fig. 1 were blacklisted (thus not assimilated) inside the geographical domain of this same figure. All other observations

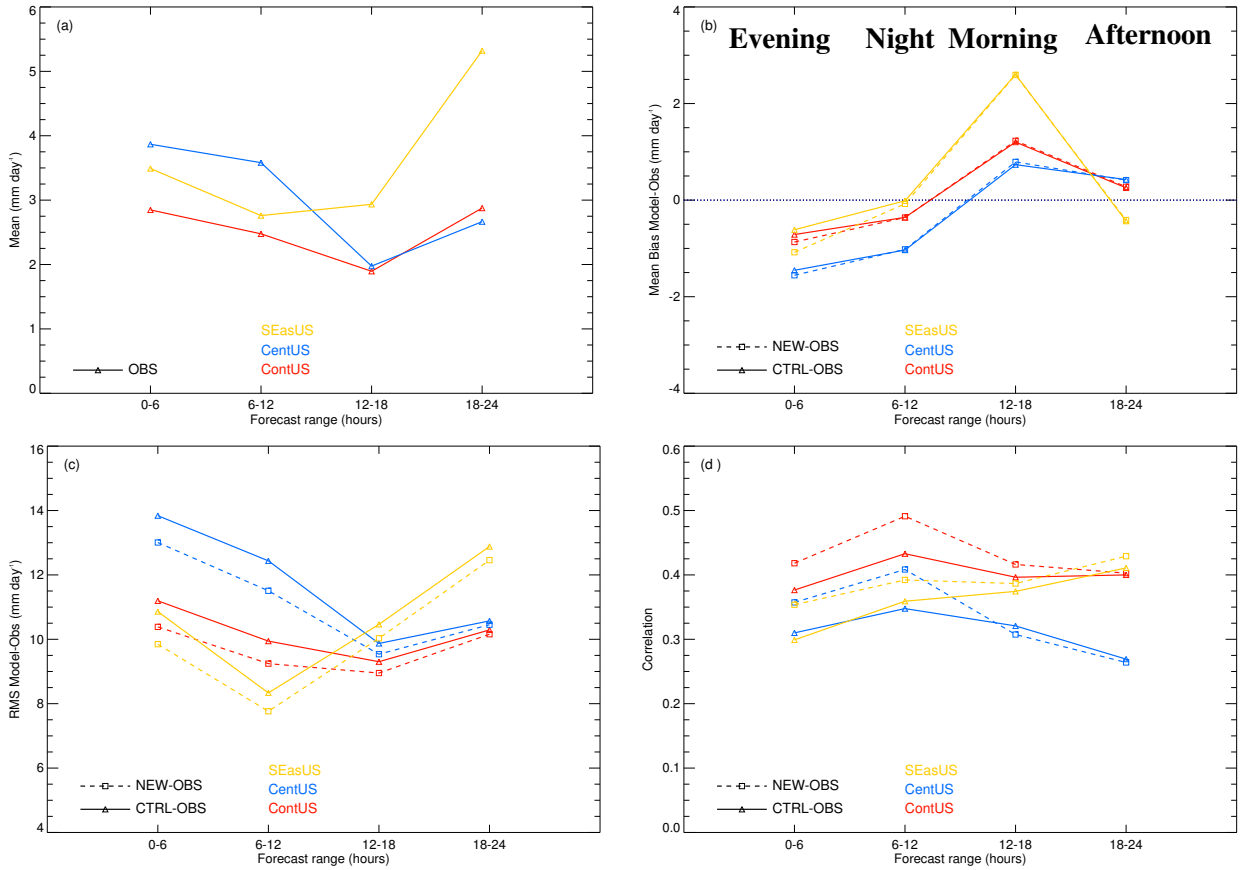


FIGURE 9: Statistics of precipitation accumulations over the US as a function of forecast range (6-hour interval up to 24h): (a) mean of NEXRAD observations, (b) mean bias of experiment minus NEXRAD, (c) mean root-mean-square differences of experiment minus NEXRAD, and (d) mean correlation coefficient between each experiment and NEXRAD. Statistics are plotted for the three domains shown in Fig. 6a (see colour legend). In panels (b) to (d), solid (resp. dashed) lines are used for CTRL (resp. NEW). Y-axis values are in mm day$^{-1}$ in panels (a) to (c) and unitless in (d). Local-time slots are indicated in panel (b).

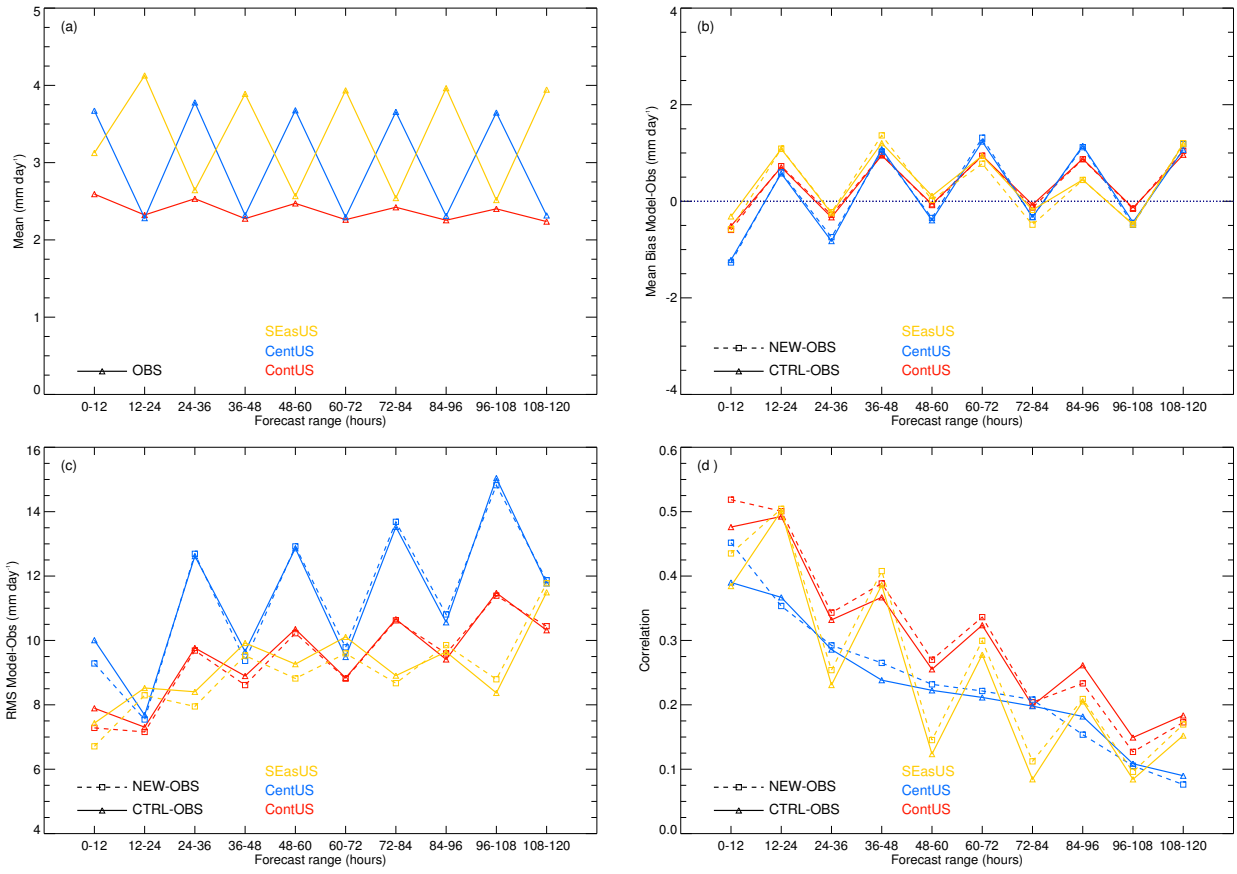


FIGURE 10: Same as in Fig. 9, but for 12-hour intervals up to 120h.

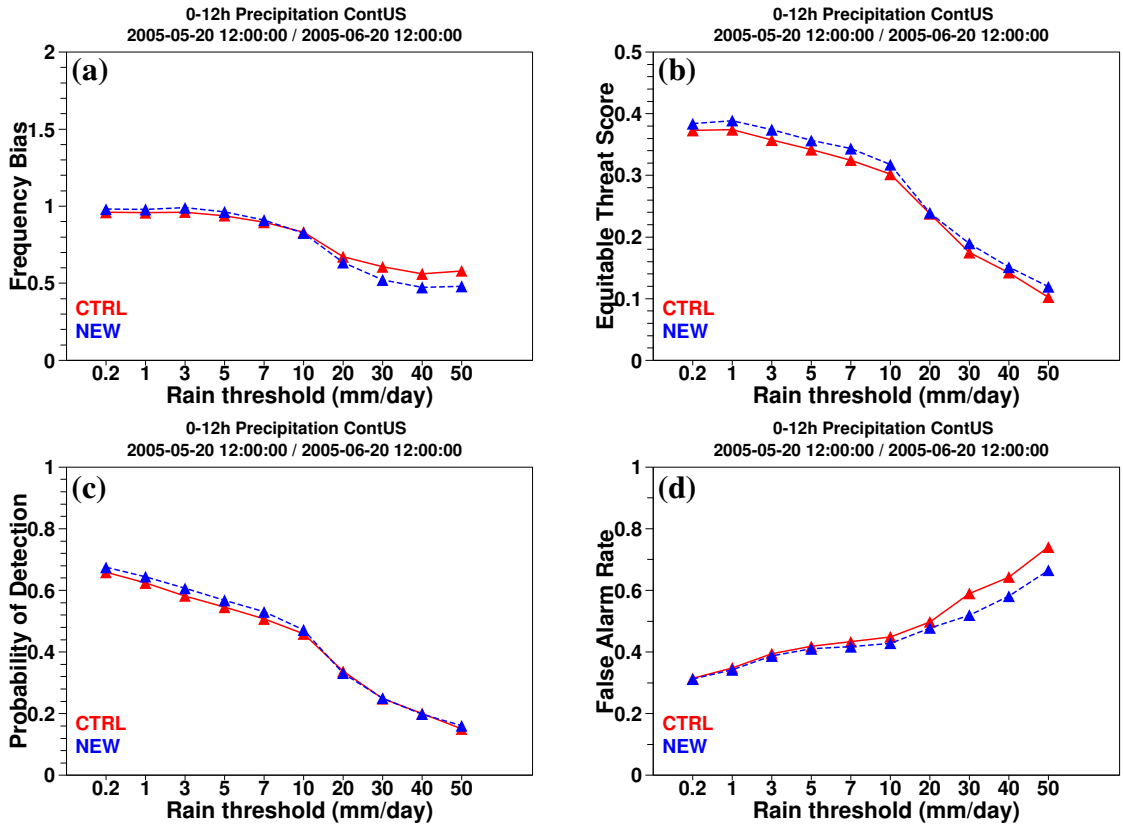


FIGURE 11: Impact of NEXRAD assimilation on model versus NEXRAD precipitation scores for the 12-h forecast and for various rainfall thresholds ranging from 0.2 to 50 mm day$^{-1}$ (x-axis): (a) frequency bias, (b) equitable threat score, (c) probability of detection and (d) false alarm rate. See Appendix 2 for the definition of each score. CTRL is shown in red, NEW in blue.

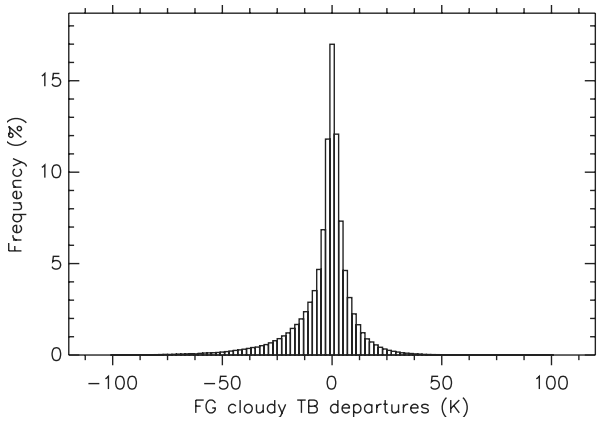


FIGURE 12: Frequency histogram of background departures w.r.t. HIRS cloudy TBs over the US from CTRL.

not related to moisture were kept inside this domain to ensure some control of the dynamics and of the mass field, whereas the standard observational coverage was kept unchanged outside the domain. This experiment (referred to as CTRL_noqUS) was run over the same month-long period as CTRL and NEW. A second experiment (NEW_noqUS hereafter) was performed, identical to CTRL_noqUS except that NEXRAD observations were also assimilated over the US. The impact of adding the NEXRAD observations as the only source of information on moisture over the US is depicted in Fig. 13 in the form of maps of mean CTRL_noqUS−CTRL and NEW_noqUS−CTRL_noqUS differences for TCWV in the 4D-Var analysis and in the 48-hour forecast. The absence of humidity observations over the US in CTRL_noqUS leads to a widespread and intense drying of the atmosphere over the eastern half of the US in the analysis (Fig. 13a). This result is consistent with those obtained by Andersson *et al.* (2006) for July 2003 after the global removal all moisture-related observations. It is remarkable that the assimilation of NEXRAD rain observations is able to produce a significant moistening over the same region (Fig. 13b), therefore correcting the analysed TCWV field towards CTRL, at least partially. As expected, these changes in TCWV are mainly confined to the rainy regions of the eastern US where NEXRAD rain observations are active. Figure 13b and d proves that the impact of the NEXRAD observations on the humidity field remains effective even after several days of model integration. As already found in section 4.2.2, the influence of NEXRAD observations on dynamical fields remains very limited. However, it is worthwhile noting that the changes in the dynamics caused by the removal of moisture observations in CTRL_noqUS are not statistically significant either compared to CTRL (not shown).

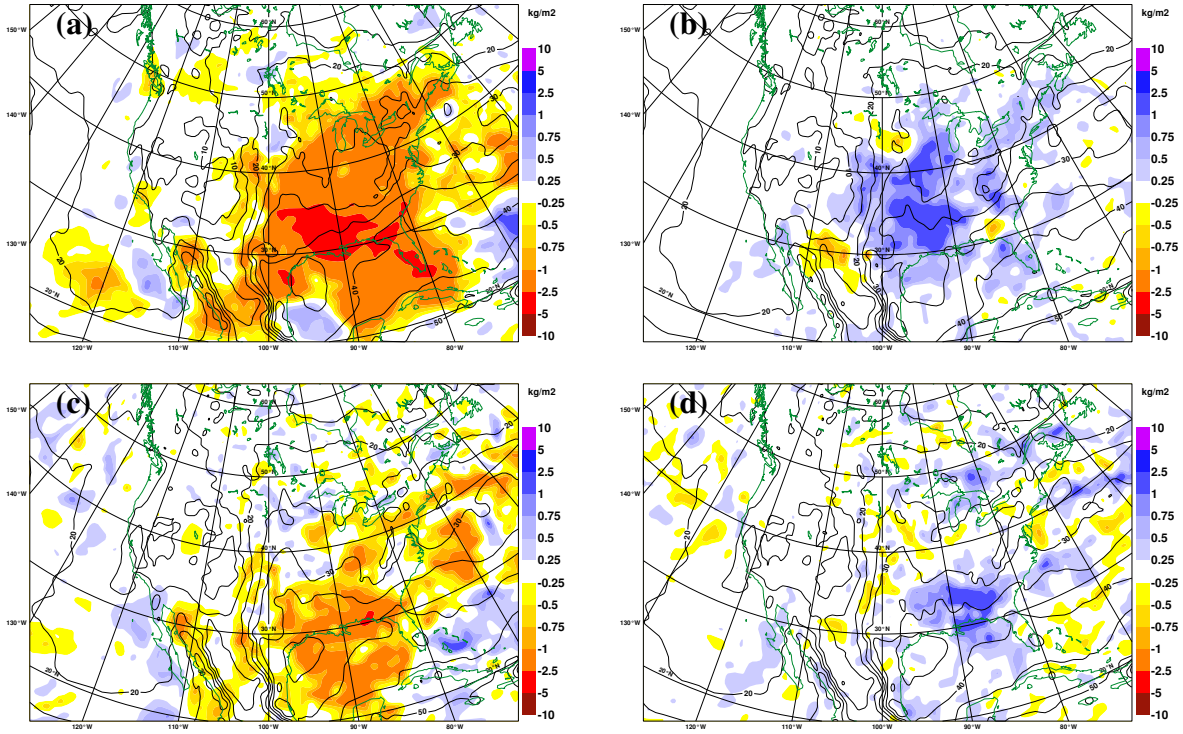


FIGURE 13: Impact of NEXRAD observations in the absence of moisture-related observations over the US. Maps of mean differences of TCWV in 4D-Var analyses (top) and 48-hour forecasts (bottom) at 0000 UTC: (a,c) CTRL_noqUS−CTRL, (b,d) NEW_noqUS−CTRL_noqUS (color shading; in kg $m^{-2}$; see text for detail on experiments). Isolines show the corresponding mean analyzed/forecasted TCWV from experiment CTRL in (a,c) and from CTRL_noqUS in (b,d) (contour interval: 5 kg $m^{-2}$).

The mean profiles of the specific humidity bias w.r.t. radiosondes (independent data in this context) in model background and analysis is also shown in Fig. 14 for CTRL_noqUS and NEW_noqUS. Figure 14 confirms that

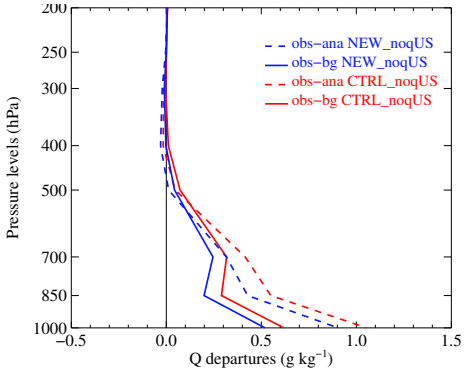


FIGURE 14: Mean vertical profiles of the specific humidity bias w.r.t. radiosondes (observation minus model) for CTRL_noqUS (red) and NEW_noqUS (blue) in the model background (solid line) and in the 4D-Var analysis (dashed line). Statistics have been computed over subdomain 24°N/50°N and 105°W/60°W. Pressure levels are in hPa and bias is in g kg$^{-1}$.

the absence of moisture observations over the US in the assimilation results in a dry bias in the background and in the analysis (up to 1.0 g kg$^{-1}$). The fact that the bias is larger in the analysis than in the background underlines the importance of including moisture-related observations to constrain the humidity analysis. More importantly, assimilating NEXRAD observations clearly helps to reduce the dry bias, which evidences that these data are consistent with radiosonde measurements. All these findings demonstrate that rain observations such as the NEXRAD data have the potential to significantly improve the quality of 4D-Var humidity analyses and subsequent forecasts in regions where other moisture-related observations are not routinely available. For instance, the assimilation of rain observations from space-borne microwave instruments (e.g. TRMM Precipitation Radar or SSMIS) might prove beneficial over the Sahel region where the ECMWF model is known to underestimate the northward extent of the summer monsoon precipitation.

Bauer *et al.* (2006a, 2006b) have demonstrated that the "1D+4D-Var" approach could be successfully applied to assimilate SSM/I rain-affected TBs in a fully operational context. This method has the advantage of offering an interesting framework for assimilating new types of observations because an efficient and flexible quality control procedure can be applied based on the 1D-Var performance in terms of convergence and linearity. This kind of refined quality control would be more difficult to apply in the context of direct 4D-Var. Nonetheless, it has become clear that some aspects of "1D+4D-Var" are not optimal. These include the fact that the background fields are used twice in the 1D-Var and the 4D-Var minimizations. To illustrate this point from this study, TCWV observation minus background departures obtained after the 1D-Var with NEXRAD data are compared to similar departures that were computed using all radiosondes that are co-located (within 100-km distance) with active NEXRAD rain observations. Calculations have been performed over 22 assimilation cycles from 0000 UTC 20 May to 1200 UTC 30 May 2005, and after applying a quality control to the radiosonde data (top pressure below 200 hPa, station altitude below 1700 m and at least 20 vertical levels available), a total of 257 co-located points were selected. A scatter plot of 1D-Var NEXRAD versus radiosonde TCWV background departures is plotted in Fig. 15. This figure indicates that the 1D-Var NEXRAD TCWV background departures are usually smaller than the radiosonde TCWV background departures though theoretically one would expect them to be comparable on average. A likely explanation for this fact is that the 1D-Var minimization produces TCWV pseudo-observations that are by construction closer to the model background state than the original NEXRAD rain observations. This strongly suggests that the extraction of information from observations that are assimilated through "1D+4D-Var" is suboptimal or, in other words, that their impact in 4D-Var analyses is likely to be underestimated.

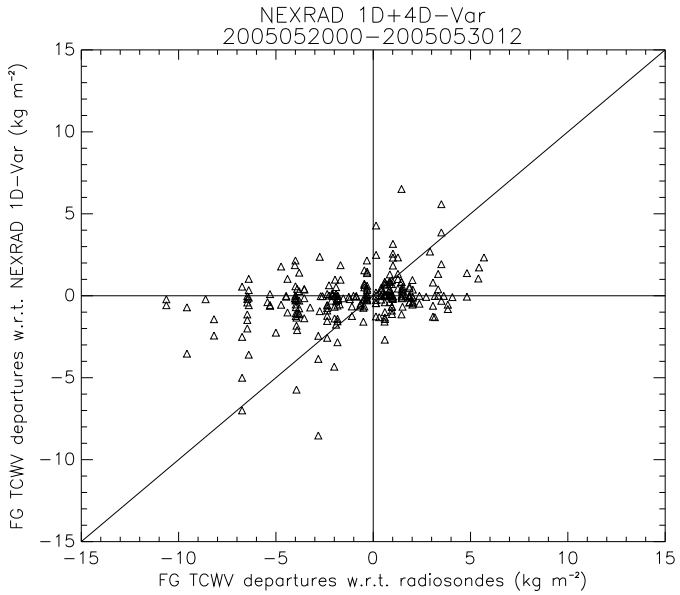


FIGURE 15: Scatter plot of 1D-Var NEXRAD versus radiosonde TCWV observation minus background departures (in kg $m^{-2}$). A total of 257 co-located points are plotted.

Despite the results from Marécal and Mahfouf's (2000) earlier study, it has often been argued that discarding temperature increments at the end of 1D-Var was too radical. Given that moist physics parameterizations used in the current version of 1D-Var are rather different from those employed by Marécal and Mahfouf (2000), a new assessment of the relevance of this simplification has been performed in the present study. To do so, the computation of analysis minus background increments of surface rain rates at the end of 1D-Var has been carried out with the inclusion of either both temperature ($T$) and specific humidity ($q$) analysis increments or $q$-increments only. Figure 16 displays a comparative scatter diagram of the results obtained from 1D-Var run on SSM/I rain rates available on 9 November 1999 between 0900 and 1500 UTC over the entire globe (11678 rainy locations used). The fact that most points are located close to the diagonal suggests that the $T$-increments do not affect very much the 1D-Var rain analysis. There are a only few points for which $T$-increments do have a significant influence. There is also a tendency for the absolute magnitude of precipitation increments to be slightly reduced when $T$-increments are discarded, which means that the final impact of rain observations is likely to be somewhat underestimated with the current "1D+4D-Var" system. It has been checked that these remarks are true regardless of the convective or stratiform nature of the situation (not shown). Note that SSM/I observations have been used here for convenience and that the conclusions are expected to be equally valid with NEXRAD observations. One can therefore conclude that neglecting $T$-increments in 1D-Var is unlikely to affect the results of the current "1D+4D-Var" significantly. However, the latter statement might be wrong for a 1D-Var system utilizing different parameterizations of moist processes.

The present "1D+4D-Var" approach is not free from other limitations. For instance, the vertical integration applied to $q$-increments to generate TCWV pseudo-observations clearly implies a loss of information that would not occur if the rain observations were directly assimilated in 4D-Var. Another limitation of the current method lies in its inadequacy to handle observations that are accumulated in time. In the present case, for instance, the assumption that NEXRAD hourly rain observations could be compared to precipitation simulated over 15-min (the model time step) had to me made. Though this hypothesis is probably not too wrong for observed hourly accumulations, it would become much more questionable should precipitation observations accumulated over longer periods of time be considered. A solution would be either to implement a "2D+4D-

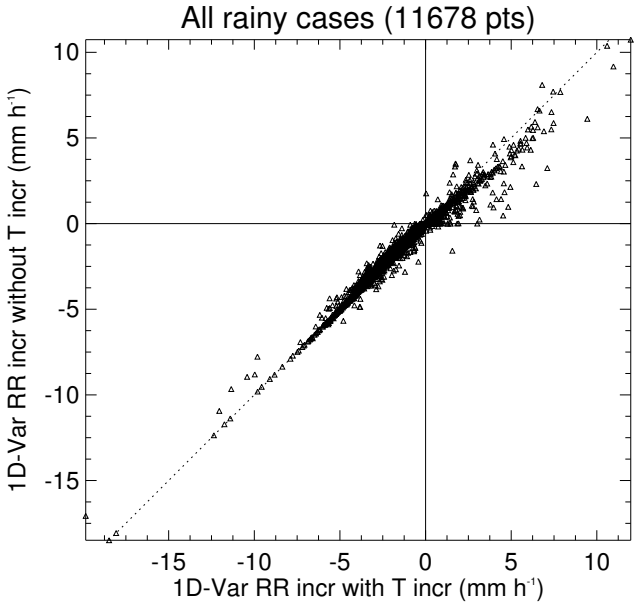


FIGURE 16: Comparison of output precipitation increments after 1D-Var when both $T$- and $q$-increments are taken into account (x-axis) and when only $q$-increments are used (y-axis). Precipitation increments are in mm day$^{-1}$). Results were obtained from 1D-Var run with SSM/I rain rates available on 9 November 1999 between 0900 and 1500 UTC over the whole globe.

Var" approach or preferably to use direct 4D-Var. All the above reasons explain why efforts are now focused on the implementation of a direct 4D-Var assimilation of observations in cloudy and rainy regions at ECMWF.

In addition to the shortcomings of the present "1D+4D-Var" approach, the lack of impact of precipitation observations on the dynamical and mass fields found in 4D-Var analyses points to the fact that the coupling between humidity and the other fields is too weak. Some interaction may develop during the model integration over the 4D-Var assimilation window especially for late observations, but a more efficient coupling between humidity and dynamical fields is missing in the current structure functions (matrix **B** in Eq. (1)). The specification of non-zero error correlations between humidity and dynamical fields (esp. divergence) as well as the inclusion of a balanced coupling between diabatic heating and vertical motion (Fillion *et al.* 2005) might alleviate the problem. Besides, current 4D-Var structure functions are perhaps inadequate to propagate increments horizontally inside or around precipitation regions. Enhancing their anisotropy according to flow characteristics would be particularly desirable in the vicinity of fronts, tropical cyclones or squall lines, for instance, but such refinement might be technically difficult to implement given the present spectral formulation of structure functions.

# 6 Conclusions

A series of "1D+4D-Var" assimilation experiments was run to assess the potential impact of assimilating NCEP Stage IV analyses of hourly accumulated surface precipitation over the US, a combination of rain-gauge and ground-based radar observations. First, the good performance of 1D-Var was successfully checked. Secondly, the validation of forecasts from the control experiment confirmed that the model strongly underpredicts the diurnal cycle of precipitation over the central regions east of the Rocky Mountains and triggers convection too early over the southeastern US, leading to an erroneous maximum of rainfall in the morning. Thirdly,

the impact of the assimilation of the additional rain observations on the 4D-Var results was studied. The moisture field was modified in the analyses and to a lesser extent in the subsequent forecasts. The impact on global scores of dynamical fields and temperature turned out to be mostly neutral with no degradation. Slight improvements of these scores were found over North America (low levels) at short ranges and over the North Atlantic (upper troposphere) and Europe (lower troposphere) later in the forecasts. Precipitation scores were positively affected for forecast ranges up to 12 hours. Additional "1D+4D-Var" experiments in which all moisture-affected observations were removed over the US, demonstrated that the NEXRAD data on their own could clearly be beneficial to the analyses and subsequent forecasts of the moisture field. This suggests that the potential impact of such precipitation observations is overshadowed by the influence of other high-quality humidity observations over land, particularly radiosondes. It also confirms that the assimilation of precipitation observations is expected to improve the quality of moisture analyses and forecasts in data sparse regions, such as West Africa where the hydrological cycle during the summer monsoon is poorly observed and simulated. It is therefore planned to run assimilation experiments over these regions using rain or reflectivity profiles obtained from the space-borne precipitation radar of TRMM and maybe data from SSMIS if the issue of surface emissivity heterogeneity can be solved.

Although Bauer *et al.* (2006a, 2006b) showed that the current "1D+4D-Var" approach works well in an operational context to assimilate SSM/I rain-affected radiances, some limitations of this method can be identified. There are some indications that the repeated use of the background fields (first in 1D-Var and then in 4D-Var) implies that the impact of precipitation observations in the final 4D-Var analyses can be underestimated. On the other hand, discarding temperature increments at the end of 1D-Var does not seem to be really problematic, at least for the set of moist physical parameterizations used. The loss of information through the vertical integration of 1D-Var specific humidity increments before 4D-Var is another potential source of suboptimality in the current method. In other respects, the 1D-Var framework does not permit the assimilation of measurements that are accumulated in time such as those from rain gauges or possibly from radars. All the above limitations should disappear when the direct 4D-Var assimilation of observations affected by rain (or clouds) becomes available.

However, further improvements are likely to be needed even in the context of direct 4D-Var. These would include the specification of more anisotropic flow-dependent background error statistics in the vicinity of cloudy regions, enhanced error correlations between moisture and other variables, and the inclusion of a coupling between increments of the vertical motion and T- and q-increments. A better definition of measurement errors and observation operator errors (including errors in moist physics parameterizations and horizontal correlations) should also be obtained.

## Acknowledgements

Marta Janisková, Anton Beljaars, Adrian Simmons, Martin Miller and Jean-Noël Thépaut should be acknowlegded for their early review of this paper. We are grateful to Martin Köhler, Andrew Orr and Peter Bechtold for their comments and suggestions during this work. We would like to thank NCEP for producing and JOSS/UCAR for providing the Stage IV precipitation observations used in this study.

## APPENDIX 1

Liste of abbreviations used in the text:

| | | |
|---|---|---|
| NOAA | = | National Oceanic And Atmospheric Administration (US) |
| NCEP | = | National Centers for Environmental Prediction (US) |
| JOSS | = | Joint Office for Science Support (US) |
| UCAR | = | University Corporation for Atmospheric Research (US) |
| JMA | = | Japan Meteorological Administration |
| ECMWF | = | European Centre for Medium-range Weather Forecasts (UK) |
| | | |
| HIRS | = | High-resolution Infrared Radiation Sounder |
| AMSU | = | Advanced Microwave Sounding Unit |
| AIRS | = | Atmospheric Infrared Sounder |
| DMSP | = | Defense Meteorological Satellite Program |
| SSM/I | = | Special Sensor Microwave Imager |
| SSMIS | = | Special Sensor Microwave Imager Sounder |
| GOES | = | Geostationary Operations Environmental Satellite |
| TRMM | = | Tropical Rainfall Measuring Mission |
| MODIS | = | Moderate Resolution Imaging Spectroradiometer |
| GPM | = | Global Precipitation Mission |

## APPENDIX 2

Precipitation scores used in this study are the Frequency Bias (FB), the Equitable Threat Score (ETS), the Probability Of Detection (POD) and the False Alarm Rate (FAR). They are defined as follows

$$FB = \frac{H+F}{H+M} \tag{5}$$

$$ETS = \frac{H-H_e}{H+M+F-H_e} \tag{6}$$

$$POD = \frac{H}{H+M} \tag{7}$$

$$FAR = \frac{F}{H+F} \tag{8}$$

where $H$ is the number of correct hits, $M$ is the number of misses and $F$ is the number of false alarms. $H_e$ is the number of correct hits purely due to random chance and is computed as

$$H_e = \frac{(H+F)(H+M)}{N} \tag{9}$$

where $N$ is the sample size.

## References

Andersson, E., Fisher, M., Hólm, E., Isaksen, L., Radnóti, G., and Trémolet, Y. (2005). Will the 4D-Var approach be defeated by nonlinearity? Technical report. ECMWF Technical Memorandum No. 479.

Andersson, E., Hólm, E., Bauer, P., Beljaars, A., Kelly, G. A., McNally, A. P., Simmons, A. J., Thépaut, J.-N., and Tompkins, A. M. (2006). Analysis and forecast impact of the main humidity observing systems. *Q. J. R. Meteorol. Soc.* submitted.

Baldwin, M. E. and Mitchell, K. E. (1996). The NCEP hourly multi-sensor U.S. precipitation analysis. In *Preprints 11th Conf. on Numerical Weather Prediction, Norfolk, VA (USA), 19–23 August 1996*, pages J95–J96.

Bauer, P., Lopez, P., Benedetti, A., Salmond, D., and Moreau, E. (2006a). Implementation of 1D+4D-Var assimilation of precipitation affected microwave radiances at ECMWF, Part I: 1D-Var. *Q. J. R. Meteorol. Soc.* in press.

Bauer, P., Lopez, P., Benedetti, A., Salmond, D., Saarinen, S., and Bonazzola, M. (2006b). Implementation of 1D+4D-Var assimilation of precipitation affected microwave radiances at ECMWF, Part II: 4D-Var. *Q. J. R. Meteorol. Soc.* in press.

Cheinet, S., Beljaars, A., Köhler, M., Morcrette, J.-J., and Viterbo, P. (2005). Assessing physical processes in the ECMWF model forecasts using the ARM SGP observations. Technical report. ECMWF-ARM Report Series, available from ECMWF, Reading, UK.

Courtier, P., Thépaut, J.-N., and Hollingsworth, A. (1994). A strategy for operational implementation of 4D-Var using an incremental approach. *Q. J. R. Meteorol. Soc.*, 120:1367–1388.

Ducrocq, V., Ricard, D., Lafore, J.-P., and Orain, F. (2002). Storm-scale numerical rainfall prediction for five precipitating events over France: On the importance of the initial humidity field. *Weather Forecast.*, 17:1236–1256.

Errico, R. M., Fillion, L., Nychka, D., and Lu, Z. Q. (2000). Some statistical considerations associated with the data assimilation of precipitation observations. *Q. J. R. Meteorol. Soc.*, 126:339–359.

Fillion, L., Tanguay, M., Ek, N., Pagé, C., and Pellerin, S. (2005). Balanced coupling between vertical motion and diabatic heating for variational data assimilation. In *Proceedings of the International Symposium on Nowcasting and Very Short Range Forecasting, WMO Workshop (WSN05), 5-9 Sept 2005, Toulouse, France*.

Fisher, M. (2004). Generalized frames on the sphere, with application to the background error covariance modelling. In *Proceedings of the ECMWF Seminar on recent developments in numerical methods for atmospheric and ocean modelling, 6-10 September 2004*, pages 87–102. Available from ECMWF, Reading, UK.

Fulton, R. A., Breidenbach, J. P., Seo, D. J., Miller, D. A., and O'Bannon, T. (1998). The WSR-88D rainfall algorithm. *Weather Forecast.*, 13:377–395.

Hou, A. Y., Zhang, S. Q., and Reale, O. (2004). Variational Continuous Assimilation of TMI and SSM/I Rain Rates: Impact on GEOS-3 Hurricane Analyses and Forecasts. *Mon. Weather Rev.*, 132:2094–2109.

Hou, A. Y., Zhang, S. Q., Silva, A. M. D., Olson, W. S., Kummerow, C. D., and Simpson, J. (2001). Improving global analysis and short-range forecast using rainfall and moisture observations derived from TRMM and SSM/I passive microwave sensors. *Bull. Am. Meteorol. Soc.*, 82:659–679.

Janisková, M., Mahfouf, J.-F., Morcrette, J.-J., and Chevallier, F. (2002). Linearized radiation and cloud schemes in the ECMWF model: Development and evaluation. *Q. J. R. Meteorol. Soc.*, 128:1505–1527.

Janisková, M., Thépaut, J.-N., and Geleyn, J.-F. (1999). Simplified and Regular Physical Parametrizations for Incremental Four-Dimensional Variational Assimilation. *Mon. Weather Rev.*, 127:26–45.

Lin, Y. and Mitchell, K. E. (2005). The NCEP Stage II/IV Hourly Precipitation Analyses: Development and Applications. In *Proceedings of the 19th AMS Conference on Hydrology, San Diego, CA (USA), 5–14 January 2005*.

Lopez, P. (2006). Cloud and Precipitation Parameterizations in Modeling and Variational Data Assimilation: A Review. *J. Atmos. Sci.* accepted.

Lopez, P., Benedetti, A., Bauer, P., Janisková, M., and Köhler, M. (2006). Experimental 2D-Var assimilation of ARM cloud and precipitation observations. *Q. J. R. Meteorol. Soc.*, 132:1325–1347.

Lopez, P. and Moreau, E. (2005). A convection scheme for data assimilation: Description and initial tests. *Q. J. R. Meteorol. Soc.*, 131:409–436.

Macpherson, B. (2001). Operational experience with assimilation of rainfall data in the Met.Office mesoscale model. *Meteorol. Atmos. Phys.*, 76:3–8.

Mahfouf, J.-F. (1999). Influence of physical processes on the tangent-linear approximation. *Tellus*, 51A:147–166.

Marécal, V. and Mahfouf, J.-F. (2000). Variational retrieval of temperature and humidity profiles from TRMM precipitation data. *Mon. Weather Rev.*, 128:3853–3866.

Marécal, V. and Mahfouf, J.-F. (2002). Four-dimensional variational assimilation of total column water vapour in rainy areas. *Mon. Weather Rev.*, 130:43–58.

Marécal, V. and Mahfouf, J.-F. (2003). Experiments on 4D-Var assimilation of rainfall data using an incremental formulation. *Q. J. R. Meteorol. Soc.*, 129:3137–3160.

Peng, S. Q. and Zou, X. (2002). Assimilation of NCEP multi-sensor hourly rainfall data using 4D-Var approach: A case study of the squall line on April 5, 1999. *Meteorol. Atmos. Phys.*, 81:237–255.

Stokes, G. M. and Schwartz, S. E. (1994). The Atmospheric Radiation Measurement (ARM) Program: programmatic background and design of the cloud and radiation test bed. *Bull. Am. Meteorol. Soc.*, 75:1201–1221.

Tompkins, A. M. and Janisková, M. (2004). A cloud scheme for data assimilation: Description and initial tests. *Q. J. R. Meteorol. Soc.*, 130:2495–2518.

Treadon, R. E. (1997). *Assimilation of satellite derived precipitation estimates within the NCEP GDAS*. PhD thesis, The Florida State University. 348 pp, available from Department of Meteorology, The Florida State University, Tallahassee, FL 32306.

Treadon, R. E., Pan, H.-L., Wu, W.-S., Lin, Y., Olson, W. S., and Kuligowski, R. J. (2002). Global and Regional Moisture Analyses at NCEP. In *Proceedings of the ECMWF Workshop on Humidity Analysis, 8-11 July 2002*, pages 33–47. Available from ECMWF, Reading, UK.

Tsuyuki, T. (1997). Variational Data Assimilation in the Tropics Using Precipitation Data. Part III: Assimilation of SSM/I Precipitation Rates. *Mon. Weather Rev.*, 125:1447–1464.

Tsuyuki, T., Koizumi, K., and Ishikawa, Y. (2002). The JMA Mesoscale 4D-Var System and Assimilation of Precipitation and Moisture Data. In *Proceedings of the ECMWF Workshop on Humidity Analysis, 8-11 July 2002*, pages 59–67. Available from ECMWF, Reading, UK.

Vukićević, T. and Bao, J. W. (1998). The Effect of Linearization Errors on 4DVAR Data Assimilation. *Mon. Weather Rev.*, 126:1695–1706.

Vukićević, T. and Errico, R. M. (1993). Linearization and adjoint of parameterized moist diabatic processes. *Tellus*, 45A:493–510.

Zou, X. (1997). Tangent linear and adjoint of "on-off" processes and their feasibility for use in 4-dimensional variational data assimilation. *Tellus*, 49A:3–31.

Zupanski, D. (1993). The effects of discontinuities in the Betts-Miller cumulus convection scheme on four-dimensional variational data assimilation. *Tellus*, 45A:511–524.